ACS Sustainable Chemistry & Engineering

Research Article

pubs.acs.org/journal/ascecg

# Promising Approach for Improving Adhesion Capacity of Foliar Nitrogen Fertilizer

Min Wang,[∥,†,‡,§] Xiao Sun,[∥,†,§] Naiqin Zhong,[⊥] Dongqing Cai,[*,†,§] and Zhengyan Wu[*,†,§]

[†]Key Laboratory of Ion Beam Bioengineering, Hefei Institutes of Physical Science, Chinese Academy of Sciences and Anhui Province, 350 Shushanhu Road, Hefei, Anhui 230031, People's Republic of China

[‡]University of Science and Technology of China, No. 96 Jinzhai Road, Hefei, Anhui 230026, People's Republic of China

[§]Bioenergy Forest Research Center of State Forestry Administration, 350 Shushanhu Road, Hefei, Anhui 230031, People's Republic of China

[⊥]Institute of Microbiology, Chinese Academy of Sciences, No. 1 Beichen West Road, Beijing 100101, People's Republic of China

*Supporting Information*

**ABSTRACT:** Foliar nitrogen fertilizer (FNF) unabsorbed by crops leaves eventually discharges into environment through rainwater washing, leaching and volatilization, causing severe pollution to water, soil and air. Therefore, improving the adhesion capacity of FNF is sorely needed. This work developed a loss-control foliar nitrogen fertilizer (LCFNF) by adding a complex, as a loss control agent (LCA), including attapulgite (ATP) irradiated by high-energy electron beam (HEEB), and straw ash-based biochar and biosilica (BCS) to traditional FNF. LCA possesses a porous micro/nano networks structure and thus could bind a large amount of nitrogen to form fertilizer-ATP-BCS system, which could be then retained by the rough surface of crop leaves. As a result, LCFNF displayed higher adhesion performance on crop leaves, lower loss amount and thus higher utilization efficiency compared with FNF. This work provides a novel and promising approach to control the loss of traditional FNF and ultimately lower the environment pollution risk.

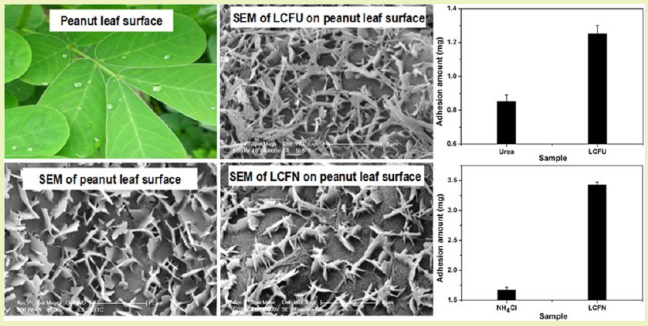


**KEYWORDS:** *Foliar nitrogen fertilizer, attapulgite, biochar and biosilica, adhesion, loss control*

## INTRODUCTION

The environmental problems associated with the overuse of nitrogen fertilizer are become increasingly severe.[1] To lower environment contamination, foliar nitrogen fertilizer (FNF) has been developed and widely applied owing to its direct uptake property and better utilization efficiency compared with root applied fertilizer.[2,3] However, the unused nitrogen on crop leaves still tends to discharge into the environment through foliar washoff and volatilization, causing environmental contamination and a waste of manpower and energy.[4−7] Therefore, there is demand to develop a new kind of FNF with higher adhesion capacity on leaf surface and lower loss amount. In this paper, we described a novel kind of FNF named loss-control foliar nitrogen fertilizer (LCFNF) by adding an appropriate amount of a complex, as a loss control agent (LCA), consisting of attapulgite (ATP) modified by high-energy electron beam (HEEB) and straw ash-based biochar and biosilica (BCS) to traditional FNF. Compared with FNF, LCFNF could effectively increase the adhesion capacity of nitrogen on crops leaves, which is favorable to control the loss of nitrogen, improve the utilization efficiency and reduce the environment pollution.

ATP ($Si_8O_{20}Mg_5(Al)(OH)_2(H_2O)_4{\cdot}4H_2O$), a kind of nanoclay, has a wide variety of applications such as paints, adsorbents, construction materials, medicine and pesticide carriers and so on, because of its nanorod structure, large specific surface area and high adsorption capacity.[8,9] However, ATP nanorods tend to aggregate with each other to form bunches, which greatly limits the application of ATP. Therefore, it is indispensable to improve the dispersibility of ATP so as to increase its properties and broaden the applications. Herein, HEEB irradiation was used to separate the ATP rods from each other to form a networks structure, and thus more nitrogen could be adsorbed on ATP effectively.

Biomass, a novel fuel for generating electricity through combustion, is gaining increasing attention due to its renewable and low pollution properties.[10,11] As a main biomass resource, plenty of straw was burned for electricity, while generating a lot of straw ash.[12] Hence, it is necessary to develop effective utilization technologies for the straw ash. Straw ash mainly consists of biochar and biosilica (BCS), which displays a micro/nanostructure with high porosity, large specific surface area and

**Received:** November 20, 2014
**Published:** February 2, 2015





DOI: 10.1021/acssuschemeng.5b00064
*ACS Sustainable Chem. Eng.* 2015, 3, 499−506

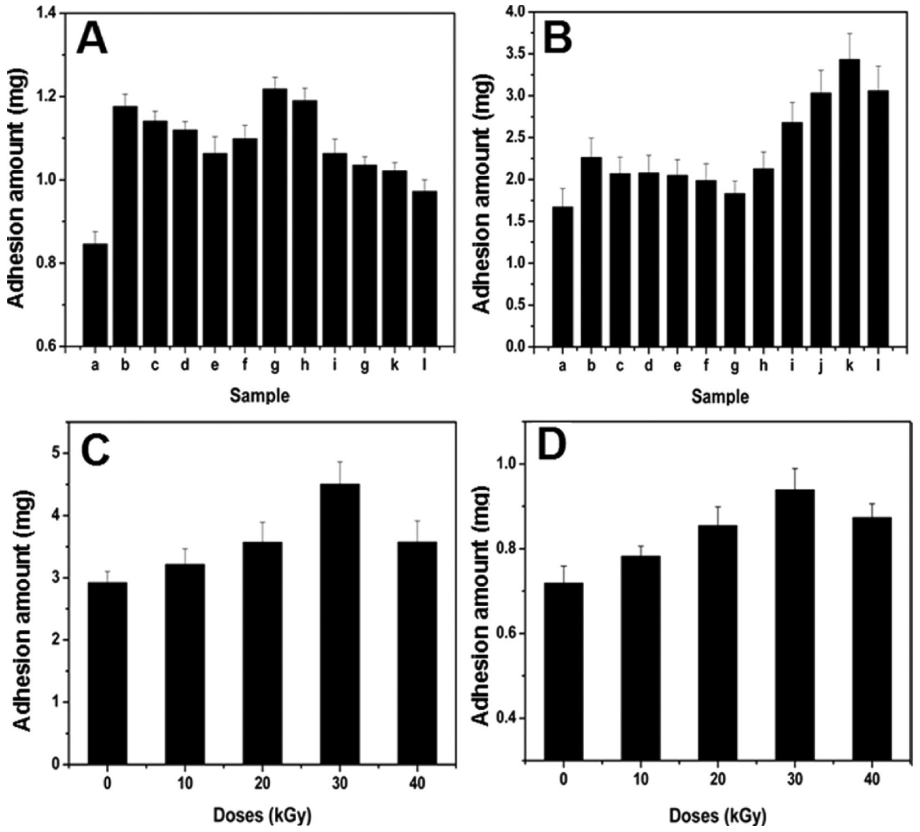


**Figure 1.** Adhesion performance of fertilizer nutrient on the peanut leaf surface. (A): (a) U, (b) U (40 g $L^{-1}$)-ATP (3 g $L^{-1}$), (c) U (40 g $L^{-1}$)-BCS (3 g $L^{-1}$), (d-l) U (40 g $L^{-1}$)-LCA (3 g $L^{-1}$, actually ATP-BCS with $W_{ATP}$:$W_{BCS}$ of 9:1, 8:1, 7:1, 6:1, 5:1, 4:1, 3:1, 2:1, 1:1, respectively). (B): (a) N (40 g $L^{-1}$), (b) N (40 g $L^{-1}$)-ATP (3 g $L^{-1}$), (c) N (40 g $L^{-1}$)-BCS (3 g $L^{-1}$), (d-l) N (40 g $L^{-1}$)-LCA (3 g $L^{-1}$, actually ATP-BCS with $W_{ATP}$:$W_{BCS}$ of 1:6, 1:5, 1:4, 1:2, 1:1, 2:1, 4:1, 5:1, 6:1, respectively). (C): U (40 g $L^{-1}$)-LCA (3 g $L^{-1}$, actually ATP-BCS with $W_{ATP}$:$W_{BCS}$ of 5:1) based on ATP irradiated by HEEB with different doses. (D): N (40 g $L^{-1}$)-LCA (3 g $L^{-1}$, actually ATP-BCS with $W_{ATP}$:$W_{BCS}$ of 6:1) based on ATP irradiated by HEEB with different doses.

negative surface charge, so that it could be used herein as an excellent carrier for FNF.[13] In addition, the micro/nanoporous structure of straw ash could be a benefit for the dispersion of ATP through the stereohindrance effect.[14,15]

The objective of this work is to develop a new FNF named LCFNF using ATP-BCS, and investigate the adhesion performance of LCFNF on crop leaves as well as the migration performance through washoff and volatilization, in comparison with FNF alone. It was found that ATP-BCS could effectively enhance the adhesion ability and reduce the loss of FNF. This work may provide not only a promising method to control FNF loss and reduce the pollution risk to environment, but also a potential utilization technology for ATP and straw ash generated in biomass power plants.

## EXPERIMENTAL SECTION

**Materials.** Natural attapulgite powder (100−200 mesh) was provided by Mingmei Co., Ltd. (Anhui, China). Straw ash-based biochar and biosilica, with approximately 60% carbon and 35% $SiO_2$ and average particle size of 10 $\mu$m, was provided by Kaidi Electric Power Co., Ltd. (Wuhan, China). Other chemicals were of analytical reagent grade and purchased from Sinopharm Chemical Reagent Company (Shanghai, China). Deionized water was used throughout this work. Peanut leaves, each with area of approximately 4 $cm^2$, were taken from experimental field of Hefei Institutes of Physical Science, Chinese Academy of Sciences.

**HEEB Irradiation.** Attapulgite samples in plastic bags (100 g each) were irradiated by high energy electron beam accelerator (10 MeV and 10 kW) with fluences of 10, 20, 30 and 40 kGy respectively at room temperature, and the resulting samples were designated as ATP10, ATP20, ATP30 and ATP40, respectively.

**Preparation of LCFNF.** ATP sample and BCS were mixed with different weight ratios. The optimum ATP-BCS complex for urea (U) (or $NH_4Cl$ (N)) was achieved through nutrients adhesion determination and designated as the LCAU (or LCAN) which was then added to U (or N), and the optimal addition amount of LCAU (or LCAN) was also obtained through the nutrients adhesion determination. Finally, LCAU (or LCAN) with the optimal amount was added to U (or N) to achieve the LCFU (or LCFN).

**Adhesion Performance Investigation.** After ultrasonic treatment (150 W, 40 kHz) for 10 min, an LCFNF suspension (1 mL) with a designated concentration was sprayed evenly onto a peanut leaf on a Petri dish with a tilt angle of 30° from the ground at 30 °C. Then, 5 mL of deionized water was sprayed evenly onto the resulting leaf to simulate the rainwater. After air-drying, the leaf was immersed into 20 mL of deionized water and shaken for 10 min at 120 rpm to wash the FNF off the leaf surface, and the concentration of FNF in deionized water was determined.

**Pot Experiments.** Soil (280 g) was placed in a pot with a trapezoidal shape, diameter of 10 cm (top) and 7 cm (bottom), and height of 7 cm. Two corn seeds were planted in the middle layer of soil (4 cm deep), and the pot stood in a dish. The system was kept in a greenhouse at 20 °C, and a total amount of 50 mL of water was sprayed on the top of the system every 4 days. After 15 days, 50 mL of urea (5 g $L^{-1}$), $NH_4Cl$ (5 g $L^{-1}$), LCFU (urea, 5 g $L^{-1}$; LCA, 0.75 g $L^{-1}$) or LCFN ($NH_4Cl$, 5 g $L^{-1}$; LCA, 0.75 g $L^{-1}$) solution was sprayed onto the surface of corn leaves in different pots, respectively. The corn heights and the chlorophyll contents of the corn leaves were investigated to obtain the promotion effects of LCFU and LCFN on the growth of corn.


DOI: 10.1021/acssuschemeng.5b00064
ACS Sustainable Chem. Eng. 2015, 3, 499−506

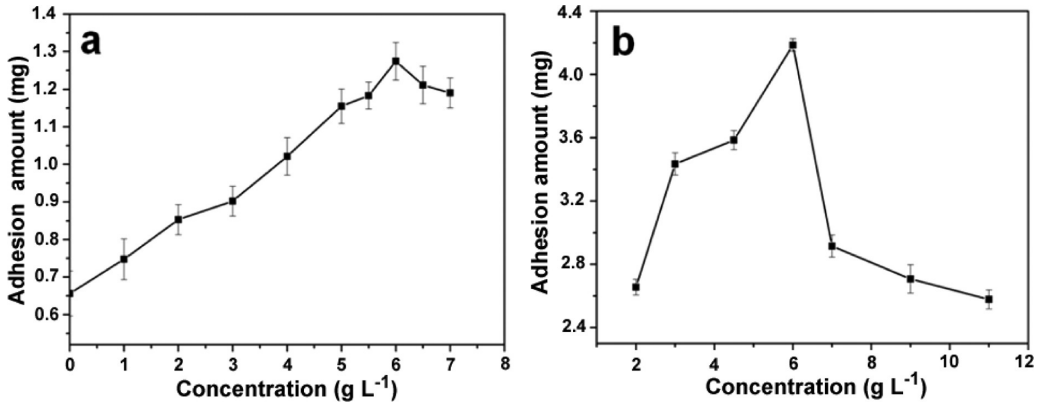


**Figure 2.** Adhesion performance of U-LCAU (a) and N-LCAN (b) with different LCAU and LCAN concentrations. The concentration of U or N solution is 40 g $L^{-1}$.

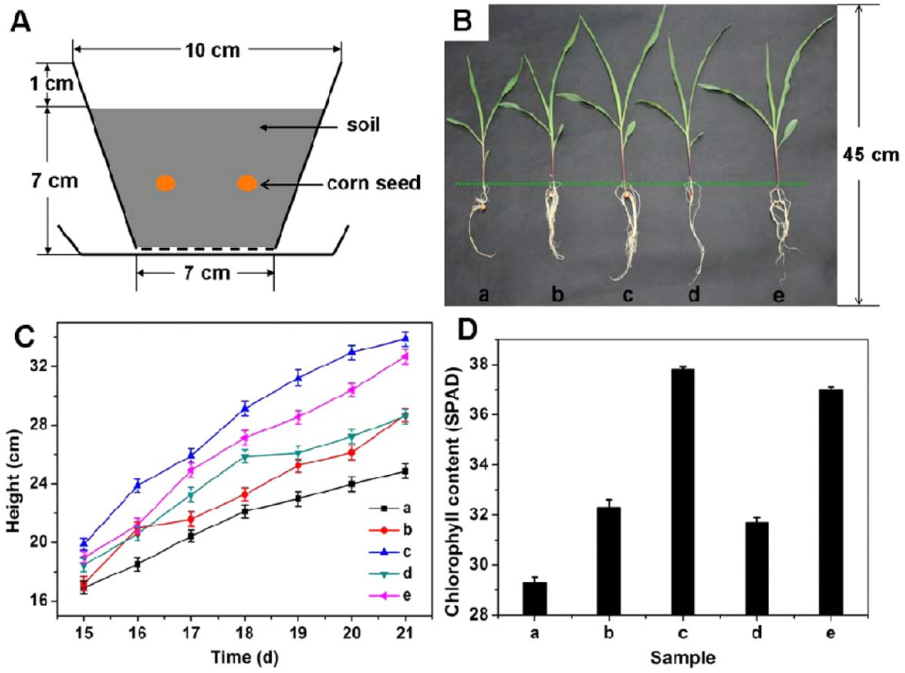


**Figure 3.** (A) Schematic diagram of the pot experiment system. (B) Digital photograph of corns. (C) Height of corn. (D) Chlorophyll contents in the leaves of corn treated with different samples: (a) blank, (b) urea, (c) LCFU, (d) $NH_4Cl$ and (e) LCFN, respectively.

**Characterization.** The morphologies of ATP, BCS, peanut leaf and LCFNF-leaf were observed with scanning electron microscopy (SEM) and energy dispersive X-ray spectroscopy (EDX) (Sirion 200, FEI Co., USA). The structure and interaction were analyzed using X-ray diffraction (XRD, TTR-III, Rigaku Co., Japan) and Fourier transform infrared spectrometry (FTIR, Bruker Co., Germany). The concentration of FNF was measured using a UV−vis spectrophotometer (UV 2550, Shimadzu Co., Japan) at a wavelength of 420 nm. The chlorophyll contents of corn leaves were determined by a chlorophyll meter (Konica Minolta Investment Ltd., Japan).

## RESULTS AND DISCUSSION

**Adhesion Performance Investigation.** The adhesion performance on the peanut leaf surface of U-ATP-BCS and N-ATP-BCS with different weight ratios of ATP to BCS were investigated compared with U and N alone. As shown in Figure 1A,B, the adhesion amounts of U-ATP (or N-ATP) and U-BCS (or N-BCS) were higher compared with U (or N) alone, indicating that ATP or BCS alone could increase the adhesion of U and N on the leaf surface. Moreover, the adhesion capacity of U-ATP-BCS (or N-ATP-BCS) was also significantly higher compared with U (or N) alone, and reached the maximum values at $W_{ATP}$:$W_{BCS}$ = 6:1 (or 5:1). This result indicated that ATP-BCS with appropriate weight ratio could exhibit much better effect on increasing the adhesion capacity of fertilizer compared with ATP or BCS alone.

It could be seen clearly in Figure 1C,D, the adhesion capacities of both U-ATP-BCS and N-ATP-BCS based on ATP irradiated by HEEB obviously increased with HEEB doses initially (0−30 kGy), reaching the maximum at 30 kGy, and then decreased after 30 kGy. That was to say, ATP30 was the most suitable for the adhesion performance of U-ATP-BCS and N-ATP-BCS compared with the raw ATP, ATP10, ATP20 and ATP40. According to our previous work,[15] owing to the thermal, physical impact and charge effects of HEEB, the dispersion and BET specific surface area (BSA) of ATP increased initially (0−30 kGy) and then decreased (30−40 kGy), achieving the maximum at 30 kGy. Therefore, the dispersion and BSA could probably play key roles in improving


DOI: 10.1021/acssuschemeng.5b00064
ACS Sustainable Chem. Eng. 2015, 3, 499−506

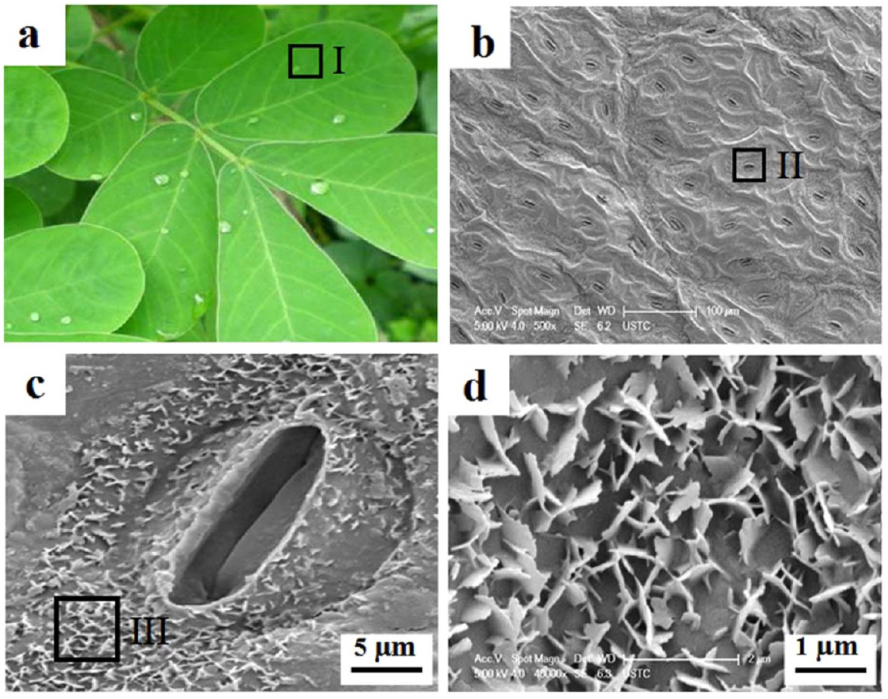


**Figure 4.** (a) Digital photo of peanut leaf; (b) SEM image of the square region marked with I in panel a; (c) SEM image with a higher magnification of the square region marked with II in panel b; (d) SEM image with a higher magnification of the square region marked with III in panel c.

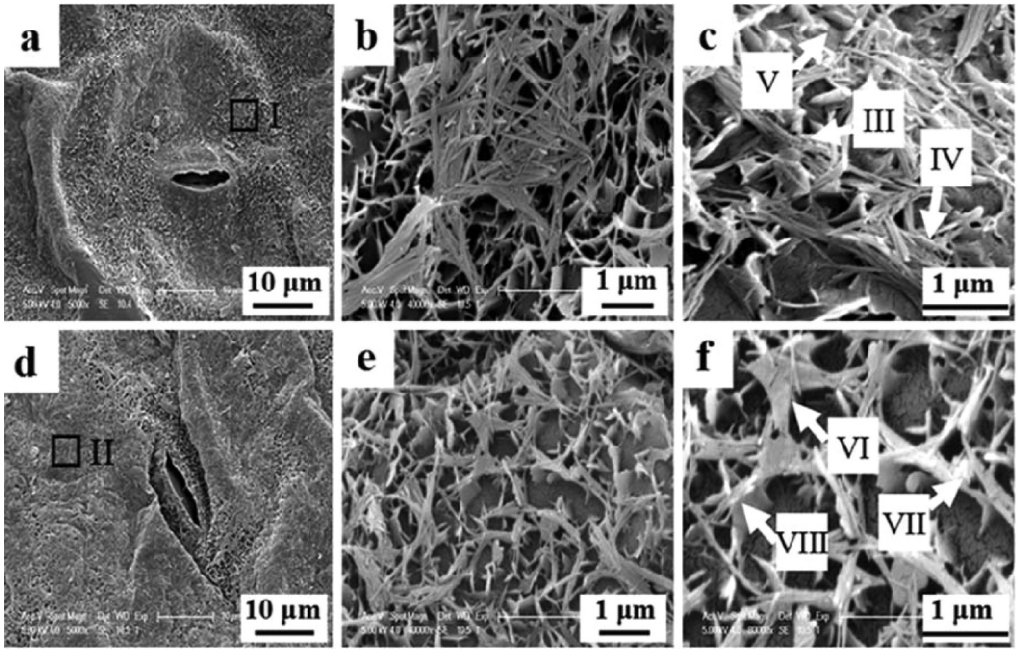


**Figure 5.** SEM images of LCAU (a–c) and LCFU (d–f) on peanut leaf surface; (b and c) magnified images of the square region marked with I; (e and f) magnified images of the square region marked with II; (III and VII) BCS; (IV) ATP; (VI and V) U; (VIII) flake. The concentration of U or N solution is 40 g $L^{-1}$.

the adhesion capacities of both U-ATP-BCS and N-ATP-BCS. In other words, the adhesion performance of LCFNF could be attributed to the adsorption ability of ATP on FNF. According to the preceding results, the optimal agent, actually the LCAU (or LCAN), for U (or N) was obtained at $W_{ATP30}$:$W_{BCS}$ = 6:1 (or $W_{ATP30}$:$W_{BCS}$ = 5:1).

To further obtain the optimum addition amount of LCAU and LCAN, the adhesion performance of U-LCAU and N-LCAN with different LCAU and LCAN concentrations was investigated. Figure 2 illustrates that the adhesion capacities of both U-LCAU and N-LCAN increased initially (0–6 g $L^{-1}$) the increasing concentration of LCAU and LCAN and then achieved the maximum at 6 g $L^{-1}$. However, the adhesion amount decreased when the LCAU (or LCAN) concentration was larger than 6 g $L^{-1}$, which was probably because LCAU (or LCAN) with high concentrations could probably form large aggregates which tended to be washed off or blown off from the leaf surface, resulting in lower adhesion performance.


DOI: 10.1021/acssuschemeng.5b00064
ACS Sustainable Chem. Eng. 2015, 3, 499–506

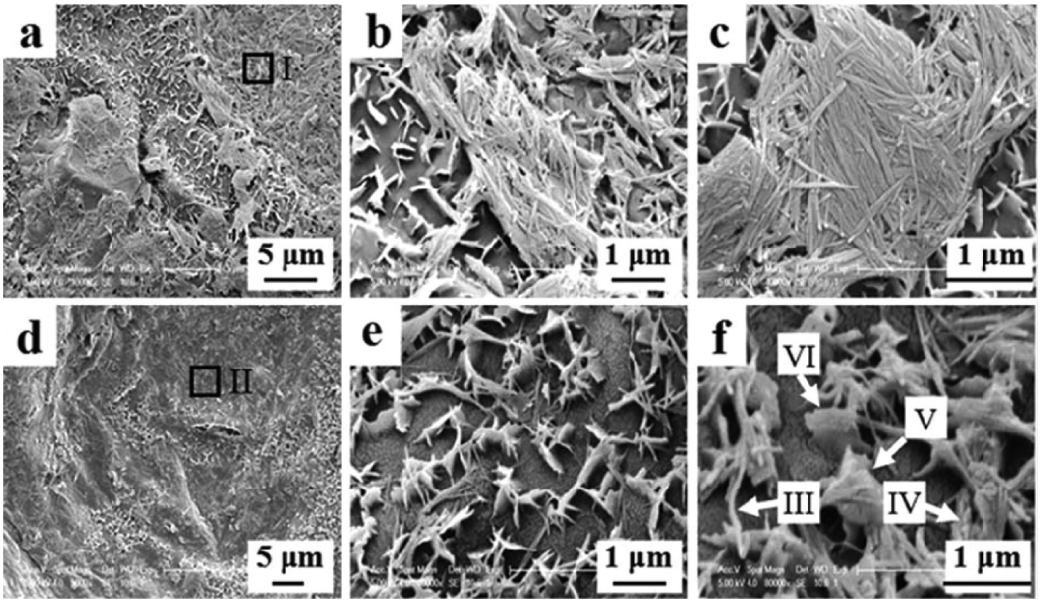


**Figure 6.** SEM images of LCAN (a–c) and LCFN (d–f) on peanut leaf surface; (b and c) magnified images of the square region marked with I; (e) and (f) magnified images of the square region marked with II; (III) N nano crystal with ATP rod as the nucleus; (IV) BCS; (V) N; (VI) flake. The concentration of U or N solution is 40 g $L^{-1}$.

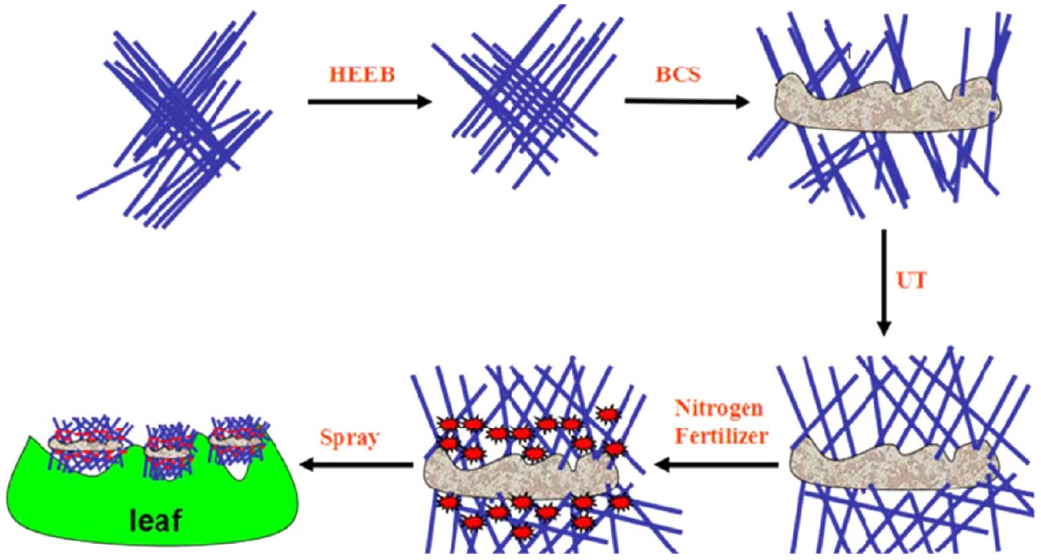


**Figure 7.** Schematic diagram showing the fabrication process of LCFNF.

Consequently, the optimal LCAU (or LCAN) concentration for U-LCAU (or N-LCAN) was 6 g $L^{-1}$. That was to say, the optimal $W_U$:$W_{LCAU}$ or $W_N$:$W_{LCAN}$ for the adhesion performance of fertilizer nutrients was 20:3. Based on the preceding analyses, the optimal U-LCAU (named as LCFU) and N-LCAN (named as LCFN) were obtained at $W_U$:$W_{ATP30}$:$W_{BCS}$ = 140:18:3 and $W_N$:$W_{ATP30}$:$W_{BCS}$ = 40:5:1, respectively.

**Effects of LCAU (or LCAN) on Corns.** As shown in Figure 3, the effects of LCAU (or LCAN) on the growth of corns were investigated through pot experiments (Figure 3A). It could be seen clearly from Figure 3B,C that LCFU (or LCFN) displayed obvious positive effects on the growth of corns during the seedling stage (15 days after seeding), resulting in higher heights and chlorophyll contents in the leaves compared with the corns treated with or without traditional FNF. That was to say, LCAU (or LCAN) could effectively increase the utilization efficiency of U (or N), which was probably attributed to the higher adhesion performance of LCFU (or LCFN) on corn leaves compared with U (or N) alone.

**Microstructure Modification Investigation.** Naturally, there are plenty of air pores (Figure 4b, c) on the peanut leaf surface (Figure 4a), and FNF nutrients could be absorbed by the leaf through these pores. Besides, a number of micro/nanoflakes (Figure 4d) could be seen clearly on the leaf surface, resulting in a rough surface. These flakes are beneficial for the adhesion of FNF through the retaining effect. However, there were still part of FNFs could not be retained by these micro/nanoflakes and those FNFs tended to discharge into environment via washing-off and volatilization. Herein, ATP-BCS composite was used as a carrier to improve the adhesion capacity of FNF, because ATP-BCS possessed porous structure (1 to 200 nm) contributing to high specific surface area (50–


DOI: 10.1021/acssuschemeng.5b00064
ACS Sustainable Chem. Eng. 2015, 3, 499–506

150 $m^2$ $g^{-1}$), high surface activity and thus could adsorb FNF into the pores or surface of ATP-BCS to form the ATP-BCS-FNF composite, which could easily be retained by the flakes on the leaf surface. Nevertheless, raw ATP tends to aggregate to form compact bunches, so ATP-BCS also shows an aggregative morphology (Figures 5a−c and 6a−c) with low dispersion and specific surface area resulting in a weakened ability to bind with FNF. In addition, raw ATP presents low adhesion performance on the leaf surface because big ATP bunches tended to fall off from the leaf under rain washing or wind blowing. In our previous work,[16] it was found that HEEB irradiation could effectively enhance the dispersion of ATP and transform ATP bunches to micro/nano networks, and the optimal fluence was 30 kGy. Therefore, ATP30-BCS was selected to further improve the adhesion capacity of FNF. As shown in Figures 5d−f and 6d−f, compared with U-ATP-BCS (or N-ATP-BCS), LCFU (or LCFN) displayed a higher dispersion, a porous micro/nanonetworks structure and a larger specific surface area. Thus, more U (or N) could be adsorbed and held in the LCAU (or LCAN) networks (Figures 5f and 6f). Meanwhile, owing to the high dispersion and networks structure, LCFU (or LCFN) could be more easily retained by the flakes on the leaf surface showing a higher adhesion capacity compared with U-ATP-BCS (or N-ATP-BCS) (Figures 5III−VIII and 6III−VI), because separated attapulgite particles could attach tightly to the micro/nano flakes on the peanut leaf surface. Interestingly, the bended nano fibers were found as shown in Figure 6III, and this indicated that N could probably crystallize, with ATP rod as the crystal nucleus, along the axial direction of ATP rod and meanwhile form fiber-shaped crystals. The formation of N crystals was also favorable for the improvement of the adhesion capacity of N.

Besides ATP, the adhesion performance of LCFNF was also dependent on the adsorption of BCS, which mainly consists of micro/nano (50−200 nm) carbon and silica particles and has a high specific surface area. Hence, FNF could effectively be adsorbed into the pores and onto the surface of BCS. Moreover, the porous structure of BCS also contributed to the dispersion of ATP because ATP could insert into the pores of BCS under UT and thus be dispersed through the stereohindrance effect (Figure 7).

**Interaction Analysis.** To further investigate the modification mechanism of HEEB irradiation on ATP, FTIR measurements were carried out. As shown in Figure 8, both ATP and ATP30 have the same characteristic peaks (987 $cm^{-1}$ for Si−O−Si and 480.2 $cm^{-1}$ for −OH translational vibration, and 1684.5 $cm^{-1}$ for −OH bending vibration), indicating that only physical interaction occurred during the irradiation process. However, the intensities of these peaks of ATP30 were much higher compared with ATP, attributed to the larger specific surface area after irradiation and thus more functional groups on ATP30. LCAU possessed the characteristic peaks of both BCS (789 $cm^{-1}$ for Si−O−Si stretching vibration, 462 $cm^{-1}$ for −OH translation and 1066 $cm^{-1}$ for Si−O stretching vibration) and ATP30, manifesting that ATP30 was successfully bound with BCS. The weakening of (Mg, Al)−OH stretching vibration at 3610 $cm^{-1}$ on ATP30 probably indicated the formation of hydrogen bonds between (Mg, Al)−OH and Si−O on BCS. Additionally, neither new peaks nor peak shifts were detected in LCAU compared with ATP30 and BCS alone, suggesting that no obvious chemical reactions occurred in the binding process between ATP30 and BCS, and the main interaction between ATP30 and BCS was a physical process.

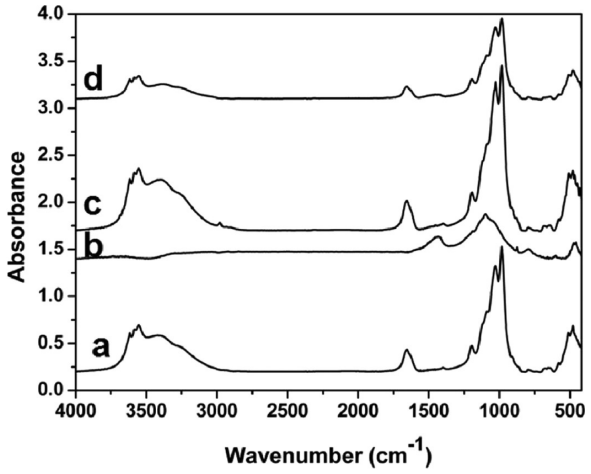


**Figure 8.** FTIR spectra of ATP (a), BCS (b), ATP30 (c) and LCAU (d).

The characteristic peaks (3450 and 3348 $cm^{-1}$ for N—H stretching vibration) of urea could be seen clearly on LCFU (Figure 9A), indicating a successful adsorption of urea onto LCAU. The peaks (3450 $cm^{-1}$ for N—H stretching vibration, 1620 $cm^{-1}$ for N—H bending vibration and 1674 $cm^{-1}$ C═O stretching vibration) of urea adsorbed onto LCAU were intensified compared with urea alone, while the peak (1121 $cm^{-1}$ for Si—O stretching vibration) of ATP30 and BCS weakened, which was probably attributed to the formation of H-bonds among −NH of urea, −OH of ATP30 and Si—O—Si of BCS. Meanwhile, other urea molecules might be adsorbed onto LCAU through electrostatic attraction. In conclusion, the main interactions between urea and LCAU could be hydrogen bonding and electrostatic attraction.

As shown in Figure 9B, the characteristic peaks of both LCAN and $NH_4Cl$ could be seen clearly on LCFN, suggesting that $NH_4Cl$ was successfully adsorbed onto LCAN. Moreover, the red shifted peaks (3037 and 3130 $cm^{-1}$ for N−H stretching vibration, 1400 $cm^{-1}$ for N−H bending vibration) of $NH_4Cl$ and the weakened peaks (486 $cm^{-1}$ for −OH translation vibration, 1090 and 1121 $cm^{-1}$ for Si−O stretching vibration) of ATP30 and BCS were probably because hydrogen bond formed among $NH_4Cl$, −OH of ATP30 or BCS, and Si−O−Si of BCS. In addition, the remaining $NH_4Cl$ might be adsorbed onto LCAN through electrostatic attraction. In a word, the main interactions between $NH_4Cl$ and LCAN were also probably hydrogen bonding and electrostatic attraction.

XRD measurements were performed to further investigate the crystal structure information on the LCAU composite. It could be seen clearly in Figure S1 (Supporting Information) that no obvious new peak or peak shift was found in ATP30 spectra compared with ATP, indicating that no obvious chemical or crystal structure change occurred during the irradiation process. Additionally, no obvious peak shift appeared on ATP30 after binding with BCS, illustrating that BCS did not intercalate the crystal layers of ATP30. Some characteristic peaks of ATP30 in LCAU in the square regions weakened compared with ATP30 alone (Figure S1e,f, Supporting Information), indicating the higher dispersion of ATP30 in LCAU. That was to say, BCS could effectively increase the dispersion of ATP30, and this corresponded to Figure 1.


DOI: 10.1021/acssuschemeng.5b00064
ACS Sustainable Chem. Eng. 2015, 3, 499−506

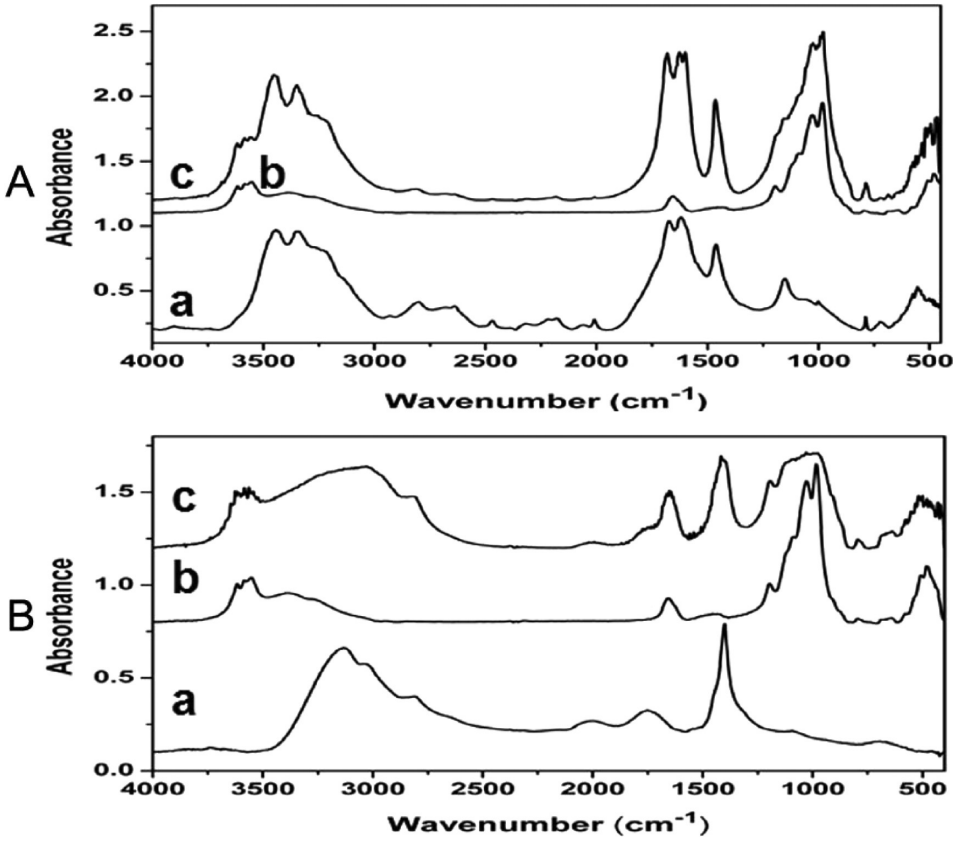


**Figure 9.** FTIR spectra. (A) urea (a), LCAU (b) and LCFU (c). (B) $NH_4Cl$ (a), LCAN (b) and LCFN (c).

It could be seen clearly in Figure S2 (Supporting Information) that LCFU possessed the characteristic peaks of both urea and LCAU, presenting that urea was successfully adsorbed onto LCAU. Additionally, the characteristic peaks of urea became weakened after binding with LCAU, which was probably because urea molecules were adsorbed into the porous structure of LCAU and thus the crystallinity of urea decreased.

As shown in Figure S3 (Supporting Information), LCFN showed the characteristic peaks of ATP30 and BCS, indicating that $NH_4Cl$ was successfully adsorbed into the pores of LCAN. Moreover, the characteristic peak (Figure S3a, Supporting Information) of $NH_4Cl$ left shifted, which was probably due to the intercalating effect of LCAN into $NH_4Cl$ crystals. That was to say, ATP30 and BCS could probably intercalate the crystal layers of $NH_4Cl$. Compared with $NH_4Cl$, some peaks (Figure S3a,b, Supporting Information) of LCFN were intensified while some peaks (Figure S3e, Supporting Information) weakened, illustrating that the crystallinity of LCFN got higher in some directions while lower in other directions. This was probably because of the formation of $NH_4Cl$ crystals in some directions with LCAN as the crystal nucleus.

Based on the preceding analysis, urea and $NH_4Cl$ could be successfully adsorbed into LCAN, and the main interactions between nitrogen and LCAN were hydrogen bonding and electrostatic attraction.

## CONCLUSION

In this paper, we developed an approach for improving the adhesion capacity and thus controlling the loss of foliar nitrogen fertilizer by adding BCS and HEEB-modified ATP to traditional foliar nitrogen fertilizer to obtain LCFNF. The results indicate that HEEB irradiation could significantly disperse ATP aggregates because of the thermal, charge and physical impact effects. In addition, BCS could further improve the dispersion of ATP through the hindrance effect. Such well dispersed ATP30-BCS possessed a porous networks structure, and thus displayed a high adsorption capacity on nitrogen and an outstanding retaining ability on the rough surface of peanut leaf. Therefore, LCFNF showed a higher adhesion capacity on peanut leaf surface compared with traditional foliar nitrogen fertilizer, which was beneficial to control the loss, improve the utilization efficiency, and ultimately decrease the environmental risk of foliar nitrogen fertilizer.

## ASSOCIATED CONTENT

### Supporting Information

XRD spectra of BCS, ATP, ATP30, LCAU, LCFU, urea, LCFN, $NH_4Cl$, and LCFN. This material is available free of charge via the Internet at http://pubs.acs.org.

## AUTHOR INFORMATION

### Corresponding Authors

*D.C. Tel.: +86-551-65595143. Fax: +86-551-65591413. E-mail: dqcai@ipp.ac.cn.

*Z.W. Tel: +86-551-65595012. Fax: +86-551-65591413. E-mail: zywu@ipp.ac.cn.

### Author Contributions

‖M.W. and X.S. are cofirst authors.

### Notes

The authors declare no competing financial interest.



DOI: 10.1021/acssuschemeng.5b00064
ACS Sustainable Chem. Eng. 2015, 3, 499−506

## ■ ACKNOWLEDGMENTS

The authors acknowledge financial support from the National Natural Science Foundation of China (No. 21407151), the Key Program of Chinese Academy of Sciences (No. KSZD-EW-Z-022-05), the Science, Technology and Service Project of Chinese Academy of Sciences (No. KFJ-EW-STS-067), the Scientific and Technological Project of Anhui Province of China (No. 1206c0805014) and the Comprehensive Agricultural Development Project of Ningxia Province of China (No. NTKJ-2014-07-02).

## ■ REFERENCES

(1) Cai, D. Q.; Wu, Z. Y.; Jiang, J.; Wu, Y. J.; Feng, H. Y.; Brown, I. G.; Chu, P. K.; Yu, Z. L. Controlling nitrogen migration through micro-nano networks. *Sci. Rep.* **2014**, *4*, 3665−3672.

(2) Finney, K. F.; Meyer, J. W.; Smith, F. W.; Fryer, H. C. Effect of foliar spraying of pawnee wheat with urea solutions on yield, protein content, and protein quality. *Agron. J.* **1957**, *49*, 341−347.

(3) Fernandez, V.; Ebert, G. Foliar iron fertilization: A critical review. *J. Plant Nutr.* **2005**, *28*, 2113−2124.

(4) Matocha, M. A.; Krutz, L. J.; Reddy, K. N.; Senseman, S. A.; Locke, M. A.; Steinriede, R. W.; Palmer, E. W. Foliar washoff potential and surface runoff losses of trifloxysulfuron in cotton. *J. Agric. Food Chem.* **2006**, *54*, 5498−5502.

(5) Zhang, Y.; Shi, R.; Rezaul, K. M.; Zhang, F.; Zou, C. Iron and zinc concentrations in grain and flour of winter wheat as affected by foliar application. *J. Agric. Food Chem.* **2010**, *58*, 12268−12274.

(6) Fernandez, V.; Rio, V.; Abadia, J.; Abadia, A. Foliar iron fertilization of peach (*Prunus persica* (L.) batsch): Effects of iron compounds, surfactants and other adjuvants. *Plant Soil* **2006**, *289*, 239−252.

(7) Fernandez, V.; Orera, I.; Abadia, J.; Abadia, A. Foliar iron fertilisation of fruit trees: Present knowledge and future perspectives − A review. *J. Hortic. Sci. Biotechnol.* **2009**, *84*, 1−6.

(8) Cai, D. Q.; Wu, Z. Y.; Jiang, J.; Ding, K. J.; Tong, L. P.; Chu, P. K.; Yu, Z. L. A unique technology to transform inorganic nanorods into nano-networks. *Nanotechnology* **2009**, *20*, 255302.

(9) Ni, B. L.; Liu, M. Z.; Lv, S. Y.; Xie, L. H.; Wang, Y. F. Multifunctional slow-release organic-inorganic compound fertilizer. *J. Agric. Food Chem.* **2010**, *58*, 12373−12378.

(10) Wu, H.; Glarborg, P.; Frandsen, F. J.; Dam-Johansen, K.; Jensen, P. A. Dust-firing of straw and additives: Ash chemistry and deposition behavior. *Energy Fuels* **2011**, *25*, 2862−2873.

(11) Srirangan, K.; Akawi, L.; Murray, M. Y.; Chou, C. P. Towards sustainable production of clean energy carriers from biomass resources. *Appl. Energy* **2012**, *100*, 172−186.

(12) Zeng, X. Y.; Ma, Y. T.; Ma, L. R. Utilization of straw in biomass energy in China. *Renewable Sustainable Energy Rev.* **2007**, *11*, 976−987.

(13) García-Jaramillo, M.; Cox, L.; Knicker, H. E.; Cornejo, J.; Spokas, K. A.; Hermosín, M. Characterization and selection of biochar for an efficient retention of tricyclazole in a flooded alluvial paddy soil. *J. Hazard. Mater.* **2015**, *286*, 581−588.

(14) Liang, B.; Lehmann, J.; Solomon, D.; Kinyangi, J.; Grossman, J.; Neill, B. O'.; Skjemstad, J. O.; Thies, J.; Luizão, F. J.; Petersen, J.; Neves, E. G. Black carbon increases cation exchange capacity in soils. *Soil Sci. Soc. Am. J.* **2006**, *70*, 1719−1730.

(15) Cai, D. Q.; Wang, L. H.; Zhang, G. L.; Zhang, X.; Wu, Z. Y. Controlling pesticide loss by natural porous micro/nano composites: Straw ash-based biochar and biosilica. *ACS Appl. Mater. Interfaces* **2013**, *5*, 9212−9216.

(16) Xiang, Y. B.; Wang, M.; Sun, X.; Cai, D. Q.; Wu, Z. Y. Controlling pesticide loss through nano networks. *ACS Sustainable Chem. Eng.* **2014**, *2*, 918−924.



DOI: 10.1021/acssuschemeng.5b00064
*ACS Sustainable Chem. Eng.* 2015, 3, 499−506